Design of Computationally Efficient FIR Filters Using Periodic Subfilters as Building Blocks

Tapio Saramäki, Tampere University of Technology, Tampere, Finland

Introduction

For many digital signal processing applications, FIR filters are preferred over their IIR counterparts as the former can be designed with exactly linear phase and they are free of stability problems and limit cycle oscillations. The major drawback of FIR filters is that they require, especially in applications demanding narrow transition bands, considerably more arithmetic operations and hardware components than do comparable IIR filters. Ignoring the correction term for very low-order filters, the minimum order of an optimum linear-phase lowpass FIR filter can be approximated by [Herrmann, Rabiner, and Chan, 1973]

$$N \approx \Phi(\delta_p, \delta_s)/(\omega_s - \omega_p), \tag{1a}$$

where

$$\begin{aligned}\Phi(\delta_p, \delta_s) =& 2\pi[0.005309(\log_{10}\delta_p)^2 + 0.07114\log_{10}\delta_p - 0.4761]\log_{10}\delta_s \\ &- 2\pi[0.00266(\log_{10}\delta_p)^2 + 0.5941\log_{10}\delta_p + 0.4278].\end{aligned} \tag{1b}$$

Here, ω_p and ω_s are the passband and stopband edge angles, whereas δ_p and δ_s are the passband and stopband ripple magnitudes. From the above estimate, it is seen that as the transition bandwidth $\omega_\mathrm{s} - \omega_p$ is made smaller, the required filter order increases inversely proportinally to it. Since the direct-form implementation exploiting the coefficient symmetry requires approximately $N/2$ multipliers, this kind of implementation becomes very costly if the transition bandwidth is small.

The cost of implementation of a narrow transition-band FIR filter can be significantly reduced by using multiplier-efficient realizations, fast convolution algorithms, or multirate filtering. This section considers those multiplier-efficient realizations that use as basic building blocks the transfer functions obtained by replacing each unit delay in a conventional transfer function by multiple delays. We concentrate on the synthesis techniques described in [Jing and Fam, 1984], [Neuvo, Dong, and Mitra, 1984], [Lim, 1986], [Saramäki, Neuvo, and Mitra 1988], [Saramäki and Fam, 1988], [Lim and Lian, 1993], and [Saramäki, 1993].

Frequency-Response Masking Approach

A very elegant approach to significantly reducing the implementation cost of an FIR filter has been proposed by Lim [Lim, 1986]. In this approach, the overall transfer function is constructed as

$$H(z) = F(z^L)G_1(z) + [z^{-LN_F/2} - F(z^L)]G_2(z), \tag{2a}$$

where

$$F(z^L) = \sum_{n=0}^{N_F} f(n)z^{-nL}, \quad f(N_F - n) = f(n), \tag{2b}$$

$$G_1(z) = z^{-M_1}\sum_{n=0}^{N_1} g_1(n)z^{-n}, \quad g_1(N_1 - n) = g_1(n), \tag{2c}$$

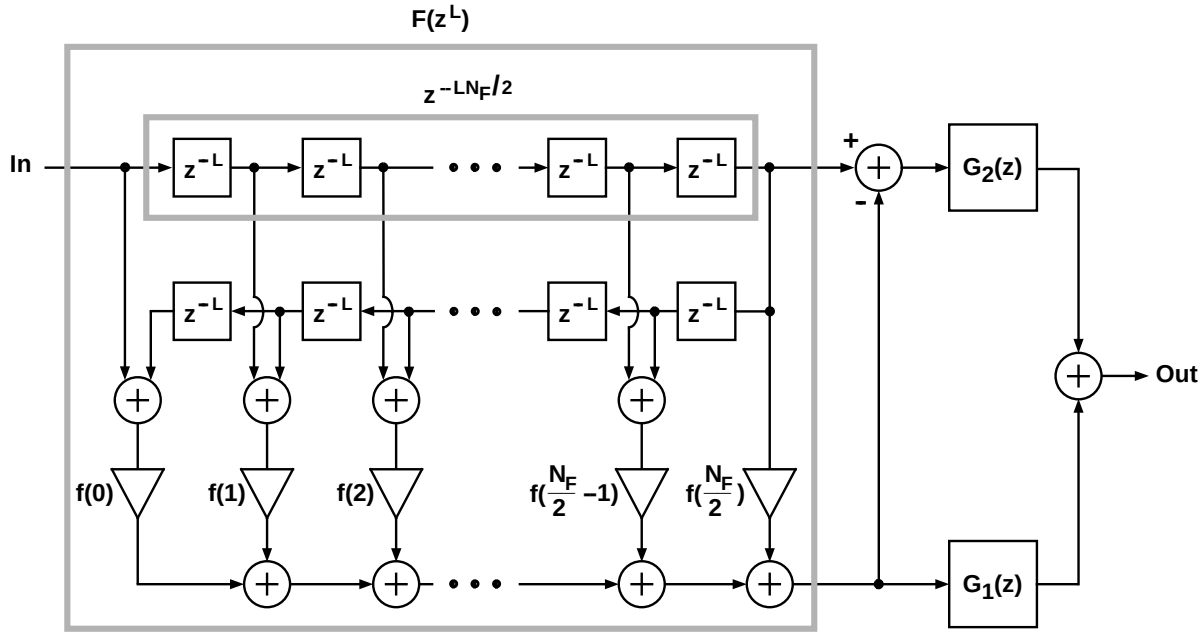

Figure 1 An efficient implementation for a filter synthesized using the frequency-response masking approach.

and

$$G_2(z) = z^{-M_2} \sum_{n=0}^{N_2} g_2(n) z^{-n}, \quad g_2(N_2 - n) = g_2(n). \tag{2d}$$

Here, N_F is even, whereas both N_1 and N_2 are either even or odd. For $N_1 \geq N_2$, $M_1 = 0$ and $M_2 = (N_1 - N_2)/2$, whereas for $N_1 < N_2$, $M_1 = (N_2 - N_1)/2$ and $M_2 = 0$. These selections guarantee that the delays of both of the terms of $H(z)$ are equal. An efficient implementation for the overall filter is depicted in Fig. 1, where the delay term $z^{-LN_F/2}$ is shared with $F(z^L)$. Also, $G_1(z)$ and $G_2(z)$ can share their delays if a transposed direct-form implementation (exploiting the coefficient symmetry) is used.

The frequency response of the overall filter can be written as

$$H(e^{j\omega}) = H(\omega) e^{-j(LN_F + \max\{N_1, N_2\})\omega/2}, \tag{3}$$

where $H(\omega)$ denotes the *zero-phase frequency response* of $H(z)$ and can be expressed as

$$H(\omega) = H_1(\omega) + H_2(\omega), \tag{4a}$$

where

$$H_1(\omega) = F(L\omega) G_1(\omega) \tag{4b}$$

and

$$H_2(\omega) = [1 - F(L\omega)] G_2(\omega) \tag{4c}$$

with

$$F(\omega) = f(N_F/2) + 2 \sum_{n=1}^{N_F/2} f(N_F/2 - n) \cos n\omega \tag{4d}$$

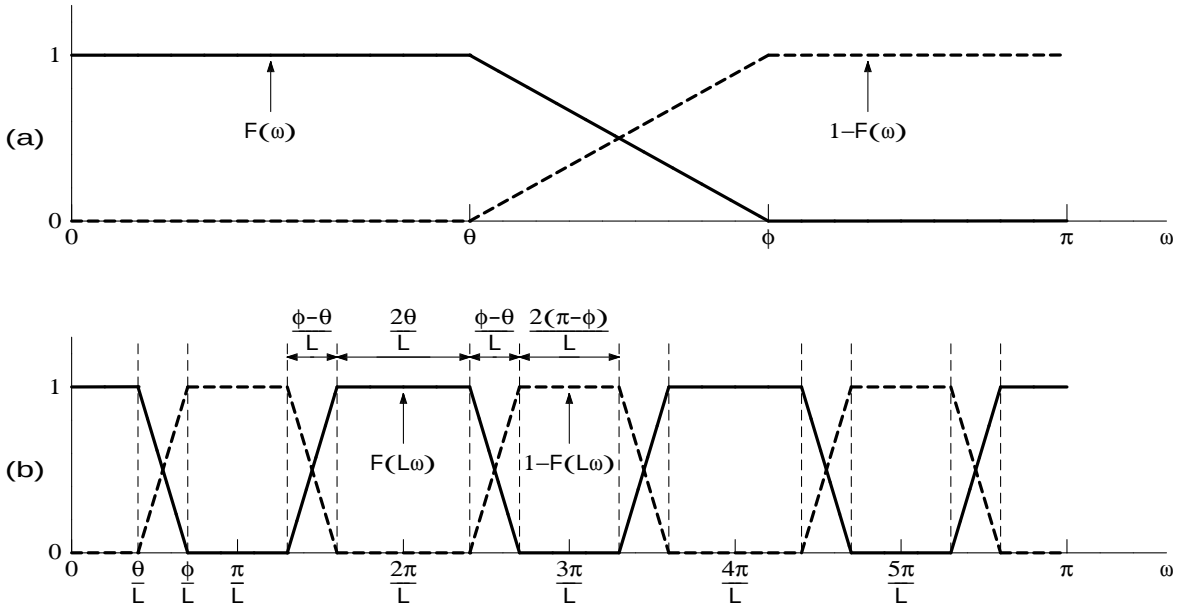

Figure 2 Generation of a complementary periodic filter pair by starting with a lowpass-highpass complementary pair. (a) Prototype filter responses $F(\omega)$ and $1 - F(\omega)$. (b) Periodic responses $F(L\omega)$ and $1 - F(L\omega)$ for $L = 6$.

and

$$G_k(\omega) = \begin{cases} g_k(N_k/2) + 2\sum_{n=1}^{N_k/2} g_k(N_k/2 - n)\cos n\omega, & N_k \text{ even} \\ 2\sum_{n=0}^{(N_k-1)/2} g_k((N_k-1)/2 - n)\cos[(n+1)\omega/2], & N_k \text{ odd} \end{cases} \tag{4e}$$

for $k = 1, 2$.

The efficiency as well as the synthesis of $H(z)$ are based on the properties of the pair of transfer functions $F(z^L)$ and $z^{-LN_F/2} - F(z^L)$, which can be generated from the pair of *prototype* transfer functions

$$F(z) = \sum_{n=0}^{N_F} f(n) z^{-n} \tag{5}$$

and $z^{-N_F/2} - F(z)$ by replacing z^{-1} by z^{-L}, that is, by substituting for each unit delay L unit delays. The order of the resulting filters is increased to LN_F, but since only every Lth impulse response value is nonzero, the filter complexity (number of adders and multipliers) remains the same. The above prototype pair forms a *complementary* filter pair since their zero-phase frequency responses, $F(\omega)$ and $1 - F(\omega)$ with $F(\omega)$ given by Eq. (4d), add up to unity. Figure 2(a) illustrates the relations between these responses in the case where $F(z)$ and $z^{-N_F/2} - F(z)$ is a lowpass-highpass filter pair with edges at θ and ϕ.

The substitution $z^{-L} \mapsto z^{-1}$ preserves the complementary property resulting in the *periodic* responses $F(L\omega)$ and $1 - F(L\omega)$, which are frequency-axis compressed versions of

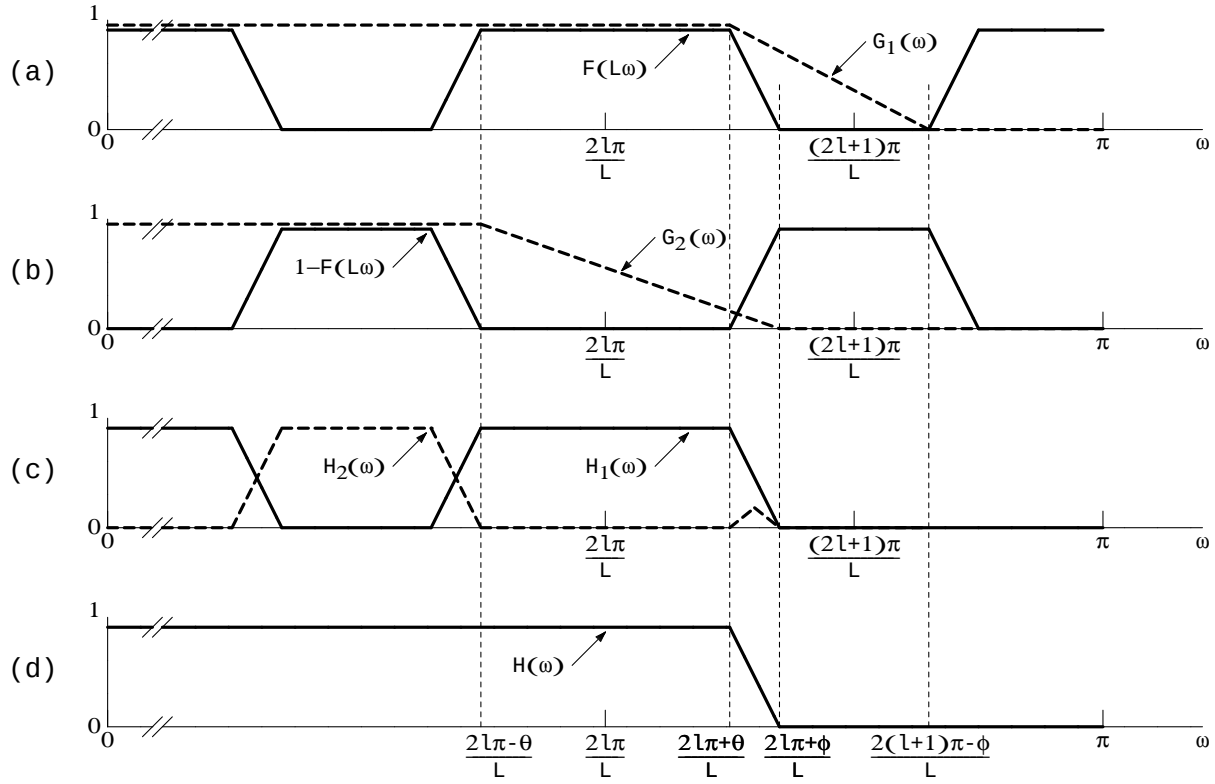

Figure 3 Case A design of a lowpass filter using the frequency-response masking technique.

the prototype responses such that the interval $[0,\ L\pi]$ is shrunk onto $[0,\ \pi]$ [see Fig. 2(b)]. Since the periodicity of the prototype responses is 2π, the periodicity of the resulting responses is $2\pi/L$ and they contain several passband and stopband regions in the interval $[0,\ \pi]$.

For a lowpass filter $H(z)$, one of the transition bands provided by $F(z^L)$ or $z^{-LN_F/2} - F(z^L)$ is used as that of the overall filter. In the first case, denoted by Case A, the edges are given by (see Fig. 3)

$$\omega_p = (2l\pi + \theta)/L, \quad \omega_s = (2l\pi + \phi)/L, \tag{6}$$

where l is a fixed integer, and in the second case, referred to as Case B, by (see Fig. 4)

$$\omega_p = (2l\pi - \phi)/L, \quad \omega_s = (2l\pi - \theta)/L. \tag{7}$$

The widths of these transition bands are $(\phi - \theta)/L$, which is only $1/L$-th of that of the prototype filters. Since the filter order is roughly inversely proportional to the transition band width, this means that the arithmetic complexity of the periodic transfer functions to provide one of the transition bands is only $1/L$-th of that of a conventional nonperiodic filter. Note that the orders of both the periodic filters and the corresponding nonperiodic filters are approximately the same, but the conventional filter does not contain zero-valued impulse response samples.

In order to exploit the attractive properties of the periodic transfer functions, the two low-order masking filters $G_1(z)$ and $G_2(z)$ are designed such that the subresponses

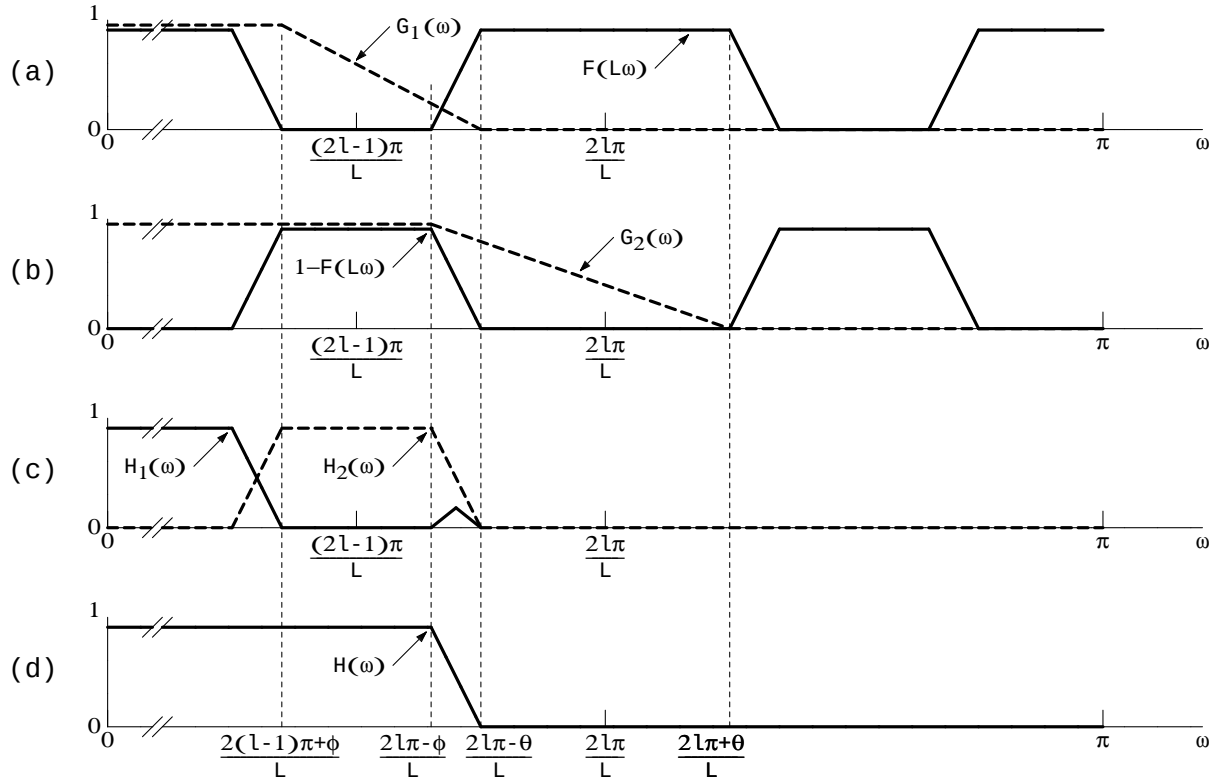

Figure 4 Case B design of a lowpass filter using the frequency-response masking technique.

$H_1(\omega)$ and $H_2(\omega)$ as given by Eqs. (4b) and (4c) approximate in the passband $F(L\omega)$ and $1 - F(L\omega)$, respectively, so that their sum approximates unity, as is desired. In the filter stopband, the role of the masking filters is to attenuate the extra unwanted passbands and transition bands of the periodic responses. In Case A, this is achieved by selecting the edges of $G_1(z)$ and $G_2(z)$ as (see Fig. 3)

$$\omega_p^{(G_1)} = \omega_p = [2l\pi + \theta]/L, \quad \omega_s^{(G_1)} = [2(l+1)\pi - \phi]/L \tag{8a}$$

$$\omega_p^{(G_2)} = [2l\pi - \theta]/L, \quad \omega_s^{(G_2)} = \omega_s = [2l\pi + \phi]/L. \tag{8b}$$

Since $F(L\omega) \approx 0$ on $[\omega_s,\ \omega_s^{(G_1)}]$, the stopband region of $G_1(z)$ can start at $\omega = \omega_s^{(G_1)}$, instead of $\omega = \omega_s$. Similarly, since $H_1(\omega) \approx F(L\omega) \approx 1$ and $[1 - F(L\omega)] \approx 0$ on $[\omega_p^{(G_2)},\ \omega_p]$, the passband region of $G_2(\omega)$ can start at $\omega = \omega_p^{(G_2)}$, instead of $\omega = \omega_p$.

For Case B designs, the required edges of the two masking filters $G_1(z)$ and $G_2(z)$ are (see Fig. 4)

$$\omega_p^{(G_1)} = [2(l-1)\pi + \phi]/L, \quad \omega_s^{(G_1)} = \omega_s = [2l\pi - \theta]/L \tag{9a}$$

$$\omega_p^{(G_2)} = \omega_p = [2l\pi - \phi]/L, \quad \omega_s^{(G_2)} = [2l\pi + \theta]/L. \tag{9b}$$

The effects of the ripples of the subresponses on the ripples of the overall response $H(\omega)$ have been studied carefully in [Lim, 1986]. Based on these observations, the design of $H(z)$

with passband and stopband ripples of δ_p and δ_s can be accomplished for both Case A and Case B in the following two steps:

1. Design $G_k(z)$ for $k = 1, 2$ using either the Remez algorithm or linear programming such that $G_k(\omega)$ approximates unity on $[0,\ \omega_p^{(G_k)}]$ with tolerance $0.85\delta_p \cdots 0.9\delta_p$ and zero on $[\omega_s^{(G_k)},\ \pi]$ with tolerance $0.85\delta_s \cdots 0.9\delta_s$.
2. Design $F(L\omega)$ such that the overall response $H(\omega)$ approximates unity on

$$\Omega_p^{(F)} = \begin{cases} \left[\omega_p^{(G_2)},\ \omega_p\right] = \left[[2l\pi - \theta]/L,\ [2l\pi + \theta]/L\right] & \text{for Case A} \\ \left[\omega_p^{(G_1)},\ \omega_p\right] = \left[[2(l-1)\pi + \phi]/L,\ [2l\pi - \phi]/L\right] & \text{for Case B} \end{cases} \tag{10a}$$

with tolerance δ_p and approximates zero on

$$\Omega_s^{(F)} = \begin{cases} \left[\omega_s,\ \omega_s^{(G_1)}\right] = \left[[2l\pi + \phi]/L,\ [2(l+1)\pi - \phi]/L\right] & \text{for Case A} \\ \left[\omega_s,\ \omega_s^{(G_2)}\right] = \left[[2l\pi - \theta]/L,\ [2l\pi + \theta]/L\right] & \text{for Case B} \end{cases} \tag{10b}$$

with tolerance δ_s.

The design of $F(L\omega)$ can be performed conveniently using linear programming [Lim, 1986]. Another, computationally more efficient, alternative is to use the Remez algorithm [Saramäki, 1993]. Its use is based on the fact that

$$|E_H(\omega)| \le 1 \quad \text{for} \quad \omega \in \Omega_p^{(F)} \cup \Omega_s^{(F)}, \tag{11a}$$

where

$$E_H(\omega) = W_H(\omega)[H(\omega) - D(\omega)] \tag{11b}$$

is satisfied when $F(\omega)$ is designed such that the maximum absolute value of the error function given in Table 1 becomes less than or equal to unity on $[0,\ \theta] \cup [\phi,\ \pi]$.

For Step 2 of the above algorithm, $D_H(\omega) = 1$ and $W_H(\omega) = 1/\delta_p$ on $\Omega_p^{(F)}$, whereas $D_H(\omega) = 0$ and $W_H(\omega) = 1/\delta_s$ on $\Omega_s^{(F)}$, giving for $k = 1, 2$

$$D_H[h_k(\omega)] = \begin{cases} 1 & \text{for } \omega \in [0,\ \theta] \\ 0 & \text{for } \omega \in [\phi,\ \pi], \end{cases} \quad W_H[h_k(\omega)] = \begin{cases} 1/\delta_p & \text{for } \omega \in [0,\ \theta] \\ 1/\delta_s & \text{for } \omega \in [\phi,\ \pi] \end{cases} \tag{12a}$$

for Case A and

$$D_H[h_k(\omega)] = \begin{cases} 1 & \text{for } \omega \in [0,\ \theta] \\ 0 & \text{for } \omega \in [\phi,\ \pi], \end{cases} \quad W_H[h_k(\omega)] = \begin{cases} 1/\delta_s & \text{for } \omega \in [0,\ \theta] \\ 1/\delta_p & \text{for } \omega \in [\phi,\ \pi] \end{cases} \tag{12b}$$

for Case B. Even though the resulting error function looks very complicated, it is straightforward to use the subroutines EFF and WATE in the Remez algorithm described in [McClellan, Parks, Rabiner, 1973] for optimally designing $F(z)$.

The order of $G_1(z)$ can be considerably reduced by allowing larger ripples on the those regions of $G_1(z)$ where $F(L\omega)$ has one of its stopbands. As a rule of thumb, the ripples on these regions can be selected to be ten times larger [Lim, 1986]. Similarly, the order

Table 1 Error Function for Designing $F(\omega)$ Using the Remez Algorithm

$$E_F(\omega) = W_F(\omega)[F(\omega) - D_F(\omega)],$$

where

$$D_F(\omega) = [u(\omega) + l(\omega)]/2, \quad W_F(\omega) = 2/[u(\omega) - l(\omega)]$$

with

$$u(\omega) = \min\Big(\Psi_1(\omega) + \psi_1(\omega), \Psi_2(\omega) + \psi_2(\omega)\Big)$$

$$l(\omega) = \max\Big(\Psi_1(\omega) - \psi_1(\omega), \Psi_2(\omega) - \psi_2(\omega)\Big)$$

$$\Psi_k(\omega) = \frac{D_H[h_k(\omega)] - G_2[h_k(\omega)]}{G_1[h_k(\omega)] - G_2[h_k(\omega)]}, \quad k = 1, 2$$

$$\psi_k(\omega) = \frac{1/W_H[h_k(\omega)]}{|G_1[h_k(\omega)] - G_2[h_k(\omega)]|}, \quad k = 1, 2$$

and

$$h_1(\omega) = (2l\pi + \omega)/L, \quad h_2(\omega) = \begin{cases} (2l\pi - \omega)/L & \text{for } \omega \in [0,\ \theta] \\ [2(l+1)\pi - \omega]/L & \text{for } \omega \in [\phi,\ \pi] \end{cases}$$

for Case A and

$$h_1(\omega) = (2l\pi - \omega)/L, \quad h_2(\omega) = \begin{cases} (2l\pi + \omega)/L & \text{for } \omega \in [0,\ \theta] \\ [2(l-1)\pi + \omega]/L & \text{for } \omega \in [\phi,\ \pi] \end{cases}$$

for Case B.

of $G_2(z)$ can be decreased by allowing (ten times) larger ripples on those regions where $F(L\omega)$ has one of its passbands.

In practical filter synthesis problems, ω_p and ω_s are given and l, L, θ, and ϕ must be determined. To ensure that Eq. (6) yields a desired solution with $0 \le \theta < \phi \le \pi$, it is required that (see Fig. 3)

$$\frac{2l\pi}{L} \le \omega_p, \quad \omega_s \le \frac{(2l+1)\pi}{L} \tag{13a}$$

for some positive integer l, giving

$$l = \lfloor L\omega_p/(2\pi) \rfloor,\ \theta = L\omega_p - 2l\pi,\ \phi = L\omega_s - 2l\pi, \tag{13b}$$

where $\lfloor x \rfloor$ stands for the largest integer which is smaller than or equal to x. Similarly, to ensure that Eq. (7) yields a desired solution with $0 \le \theta < \phi \le \pi$, it is required that (see Fig. 4)

$$\frac{(2l-1)\pi}{L} \le \omega_p, \quad \omega_s \le \frac{2l\pi}{L} \tag{14a}$$

for some positive integer l, giving

$$l = \lceil L\omega_s/(2\pi) \rceil,\ \theta = 2l\pi - L\omega_s,\ \phi = 2l\pi - L\omega_p, \tag{14b}$$

where $\lceil x \rceil$ stands for the smallest integer which is larger than or equal to x. For any set of ω_p, ω_s, and L, either Eq. (13b) or Eq. (14b) (not both) will yield the desired θ and ϕ, provided that L is not too large. If $\theta = 0$ or $\phi = \pi$, then the resulting specifications for $F(\omega)$ are meaningless and the corresponding value of L cannot be used.

The remaining problem is to determine L to minimize the number of multipliers, which is $N_F/2 + 1 + \lfloor (N_1 + 2)/2 \rfloor + \lfloor (N_2 + 2)/2 \rfloor$ or $N_F + N_1 + N_2 + 3$ depending on whether the symmetries in the filter coefficients are exploited or not. Hence, in both cases, a good measure of the filter complexity is the sum of the orders of the subfilters. Instead of determining the actual minimum filter orders for various values of L, the computational workload can be significantly reduced based on the use of the estimation formula given by Eq. (1). Since the widths of transition bands of $F(z)$, $G_1(z)$, and $G_2(z)$ are $\phi - \theta$, $(2\pi - \phi - \theta)/L$, and $(\phi + \theta)/L$, respectively, good estimates for the corresponding filter orders are

$$N_F \approx \frac{\Phi(\delta_p, \delta_s)}{\phi - \theta}, \quad N_1 \approx \frac{L\Phi(\delta_p, \delta_s)}{2\pi - \phi - \theta}, \quad N_2 \approx \frac{L\Phi(\delta_p, \delta_s)}{\phi + \theta}. \tag{15}$$

For the optimum nonperiodic direct-form design, the transition bandwidth is $\omega_s - \omega_p = (\phi - \theta)/L$, giving

$$N_{\text{opt}} \approx \frac{L\Phi(\delta_p, \delta_s)}{\phi - \theta}. \tag{16}$$

The sum of the subfilter orders can be expressed in terms of N_{opt} as follows

$$N_{\text{ove}} = N_{\text{opt}} \left[\frac{1}{L} + \frac{\phi - \theta}{2\pi - \phi - \theta} + \frac{\phi - \theta}{\phi + \theta} \right]. \tag{17}$$

The smallest values of N_{ove} are typically obtained at those values of L for which $\theta + \phi \approx \pi$ and, correspondingly, $2\pi - \theta - \phi \approx \pi$. In this case, $N_1 \approx N_2$ and Eq. (17) reduces, after substituting $\phi - \theta = L(\omega_s - \omega_p)$, to

$$N_{\text{ove}} = N_{\text{opt}} \left[\frac{1}{L} + 2L(\omega_s - \omega_p)/\pi \right]. \tag{18}$$

At these values of L, N_F decreases and $N_1 \approx N_2$ increases inversely proportionally to L with the minimum of N_{ove},

$$N_{\text{ove}} = 2N_{\text{opt}} \sqrt{\frac{2(\omega_s - \omega_p)}{\pi}}, \tag{19}$$

taking place at

$$L_{\text{opt}} = 1 \Big/ \sqrt{\frac{2(\omega_s - \omega_p)}{\pi}} \ . \tag{20}$$

If for $L = L_{\text{opt}}$, $\theta + \phi$ is not approximately equal to π, then L minimizing the filter complexity can be found in the near vicinity of L_{opt}. The following example illustrates the use of the above estimation formulas.

Example 1: Consider the specifications: $\omega_p = 0.4\pi$, $\omega_s = 0.402\pi$, $\delta_p = 0.01$, and $\delta_s = 0.001$. For the optimum conventional direct-form design, $N_{\text{opt}} = 2541$, requiring 1271 multipliers when the coefficient symmetry is exploited. Eq. (20) gives $L_{\text{opt}} = 16$. Table

Table 2 Estimated Filter Orders for the Admissible Values of L in the Vicinity of $L_{\text{opt}} = 16$

L	Case	l	θ	ϕ	N_F	N_1	N_2	$N_F + N_1 + N_2$
8	B	2	0.784π	0.8π	318	98	26	442
9	B	2	0.382π	0.4π	282	38	58	378
11	A	2	0.4π	0.422π	232	47	69	348
12	A	2	0.8π	0.824π	212	162	38	412
13	B	3	0.774π	0.8π	196	155	43	394
14	B	3	0.372π	0.4π	182	58	92	332
16	A	3	0.4π	0.432π	160	70	98	328
17	A	3	0.8π	0.834π	150	236	54	440
18	B	4	0.764π	0.8π	142	210	58	410
19	B	4	0.362π	0.4π	134	78	128	340
21	A	4	0.4π	0.442π	122	92	128	342
22	A	4	0.8π	0.844π	116	314	68	498

2 shows, for the admissible values of L in the vicinity of this value, l, θ, ϕ, the estimated orders for the subfilter, and the sum of the subfilter orders as well as whether the overall filter is a Case A or Case B design. For N_F, the minimum even order larger than or equal to the estimated order is used, whereas N_2 is forced even (odd) if N_1 is even (odd).

Also with the estimated filter orders of Table 2, $L = 16$ gives the best result. The actual filter orders are $N_F = 162$, $N_1 = 70$, and $N_2 = 98$. The responses of the subfilters as well as that of the overall design are depicted in Fig. 5. The overall number of multipliers and adders for this design are 168 and 330, respectively, which are 13 % of those required by an equivalent conventional direct-form design (1271 and 2541). The overall filter order is 2690, which is only 6 % higher than that of the direct-form design (2541).

Multistage Frequency-Response Masking Approach

If the order of $F(z)$ is too high, its complexity can be reduced by implementing it using the frequency-response masking technique. Extending this to an arbitrary number of stages results in the multistage frequency-response masking approach [Lim, 1986], [Lim and Lian, 1993], where $H(z)$ is generated iteratively as

$$H(z) \equiv F^{(0)}(z) = F^{(1)}(z^{L_1})G_1^{(1)}(z) + [z^{-L_1 N_F^{(1)}/2} - F^{(1)}(z^{L_1})]G_2^{(1)}(z) \tag{21a}$$

$$F^{(1)}(z) = F^{(2)}(z^{L_2})G_1^{(2)}(z) + [z^{-L_2 N_F^{(2)}/2} - F^{(2)}(z^{L_2})]G_2^{(2)}(z) \tag{21b}$$

$$\vdots \quad \vdots \quad \vdots$$

$$F^{(R-1)}(z) = F^{(R)}(z^{L_R})G_1^{(R)}(z) + [z^{-L_R N_F^{(R)}/2} - F^{(R)}(z^{L_R})]G_2^{(R)}(z). \tag{21c}$$

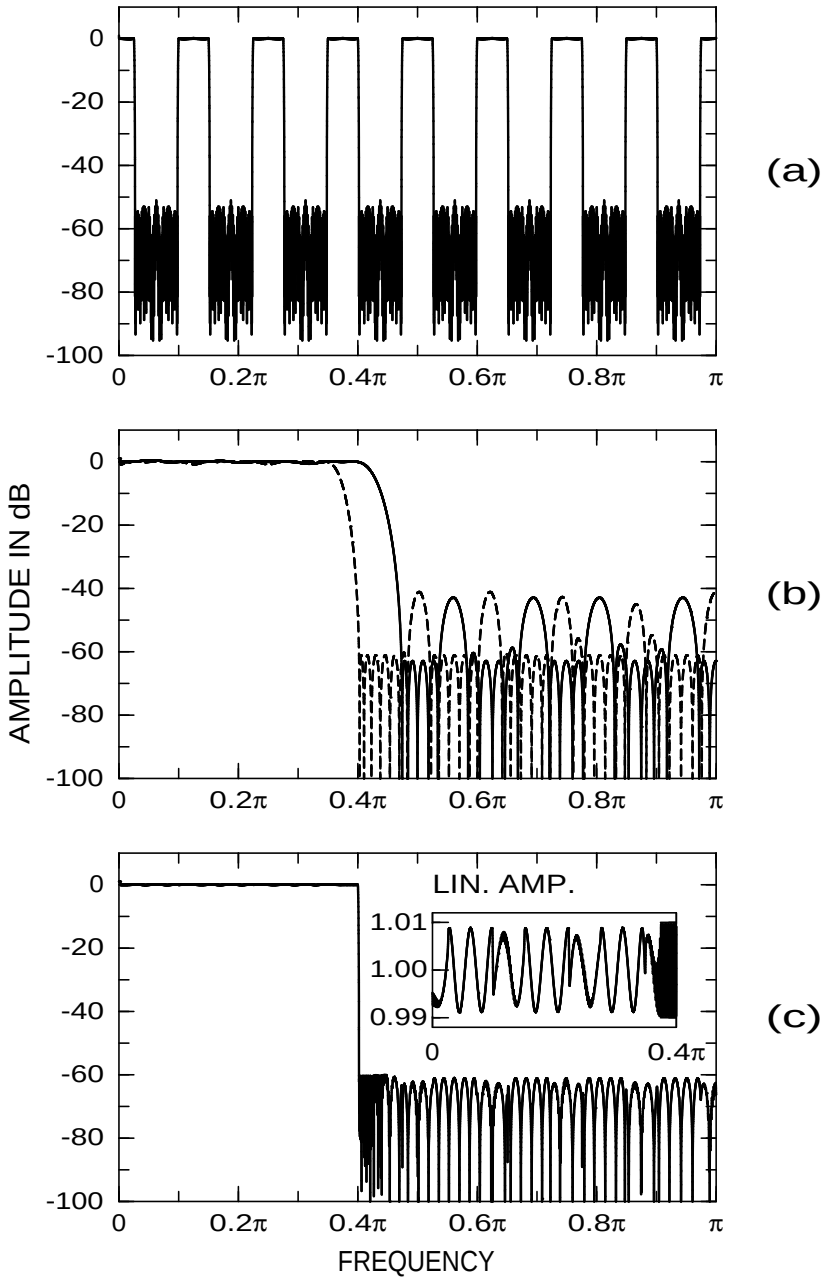

Figure 5 Amplitude responses for a filter synthesized using the frequency-response masking approach. (a) Periodic response $F(L\omega)$. (b) Responses $G_1(\omega)$ (solid line) and $G_2(\omega)$ (dashed line). (c) Overall response.

Here, the $G_1^{(r)}(z)$'s and $G_2^{(r)}(z)$'s for $r = 1, 2, \cdots, R$ as well as $F^{(R)}(z)$ are the filters to be designed. For implementation purposes, $H(z)$ can be expressed in the form shown in Table 3. Figure 6 shows an efficient implementation for a three-stage filter, where the delay terms z^{-M_3}, z^{-m_2}, and z^{-m_1} can be shared with $F^{(3)}(z^{\widehat{L}_3})$. In order to obtain a desired overall solution, the orders of the $G_1^{(r)}(z)$'s and $G_2^{(r)}(z)$'s for $r = 2, 3, \cdots, R$, denoted by $N_1^{(r)}$ and

Table 3 Implementation Form for the Transfer Function in the Multistage Frequency-Response Approach

$$H(z) \equiv F^{(0)}(z^{\widehat{L}_0}) = F^{(1)}(z^{\widehat{L}_1})G_1^{(1)}(z^{\widehat{L}_0}) + [z^{-M_1} - F^{(1)}(z^{\widehat{L}_1})]G_2^{(1)}(z^{\widehat{L}_0})$$

$$F^{(1)}(z^{\widehat{L}_1}) = F^{(2)}(z^{\widehat{L}_2})G_1^{(2)}(z^{\widehat{L}_1}) + [z^{-M_2} - F^{(2)}(z^{\widehat{L}_2})]G_2^{(2)}(z^{\widehat{L}_1})$$

$$\vdots \quad \vdots \quad \vdots$$

$$F^{(R-1)}(z^{\widehat{L}_{R-1}}) = F^{(R)}(z^{\widehat{L}_R})G_1^{(R)}(z^{\widehat{L}_{R-1}}) + [z^{-M_R} - F^{(R)}(z^{\widehat{L}_R})]G_2^{(R)}(z^{\widehat{L}_{R-1}}),$$

where

$$\widehat{L}_0 = 1, \quad \widehat{L}_r = \prod_{k=1}^{r} L_k, \quad r = 1, 2, \cdots, R$$

$$M_R = \widehat{L}_R N_F^{(R)}/2, \quad M_{R-r} = M_{R-r+1} + m_{R-r}, \quad r = 1, 2, \cdots, R-1$$

$$m_{R-r} = \widehat{L}_{R-r} \max\{N_1^{(R-r+1)}, N_2^{(R-r+1)}\}/2, \quad r = 1, 2, \cdots, R-1$$

$N_F^{(R)}$ is the order of $F^{(R)}(z)$.

$N_1^{(r)}$ and $N_2^{(r)}$ are the orders of $G_1^{(r)}(z)$ and $G_2^{(r)}(z)$, respectively.

$N_2^{(r)}$ in Table 3, have to be even.

Given the filter specifications and the L_r's for $r = 1, 2, \cdots, R$, the $G_1^{(r)}(z)$'s and $G_1^{(r)}(z)$'s as well as $F^{(R)}(z)$ can be synthesized in the following steps:

1. Set $r = 1$, $L = L_1$, and
$$D_H(\omega) = \begin{cases} 1 & \text{for } \omega \in [0,\ \omega_p] \\ 0 & \text{for } \omega \in [\omega_s,\ \pi], \end{cases} \quad W_H(\omega) = \begin{cases} 1/\delta_p & \text{for } \omega \in [0,\ \omega_p] \\ 1/\delta_s & \text{for } \omega \in [\omega_s,\ \pi]. \end{cases} \tag{22}$$
2. Determine whether $F^{(r-1)}(z)$ is a Case A or Case B design as well as θ, ϕ, and l for $F^{(r)}(z)$ according to Eq. (13b) or (14b). Also, determine $\omega_p^{(G_k)}$ and $\omega_p^{(G_k)}$ for $k = 1, 2$ from Eq. (8) or (9).
3. Design $G_k^{(r)}(z)$ for $k = 1, 2$ using either the Remez algorithm or linear programming, in such a way that
$$\max_{\omega \in [0,\ \omega_p^{(G_k)}] \cup [\omega_s^{(G_k)},\ \pi]} |W_H(\omega)[G_k^{(r)}(\omega) - D_H(\omega)]| \le 0.9. \tag{23}$$
4. Determine $W_F(\omega)$ and $D_F(\omega)$ from Table 1.
5. If $r = R$, then go to the next step. Otherwise, set $r = r + 1$, $L = L_r$, $W_H(\omega) = W_F(\omega)$, $D_H(\omega) = D_F(\omega)$, $\omega_p = \theta$, $\omega_s = \phi$, and go to Step 2.

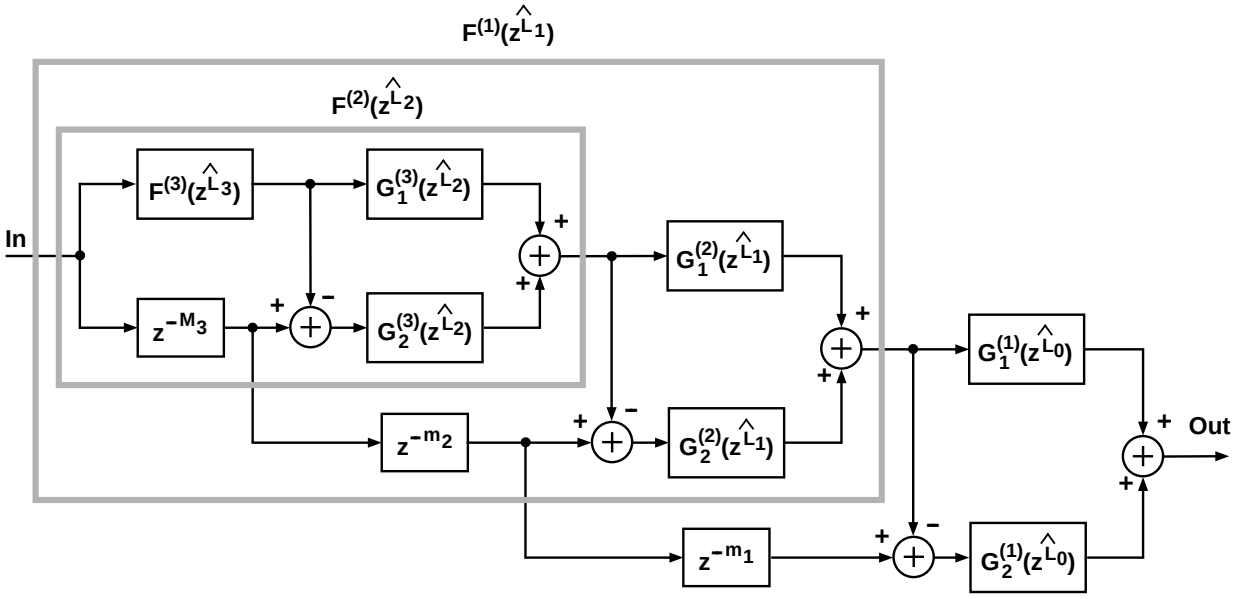

Figure 6 An implementation for a filter synthesized using the three-stage frequency-response masking approach.

6. Design $F^{(R)}(z)$, using either the Remez algorithm or linear programming, in such a way that

$$\max_{\omega \in [0,\ \theta] \cup [\phi,\ \pi]} |W_F(\omega)[F^{(R)}(\omega) - D_F(\omega)]| \leq 1. \tag{24}$$

In the above algorithm, $G_1^{(1)}(z)$ and $G_2^{(1)}(z)$ are determined like in the one-stage frequency-response masking technique. The remaining filter part as given by Eq. (21b) has then to be designed such that the maximum absolute value of the error function given in Table 1 becomes less than or equal to unity on $[0,\ \theta] \cup [\phi,\ \pi]$. Using the substitutions $\omega_p = \theta$ and $\omega_s = \phi$, the synthesis problem for $F^{(1)}(z)$ becomes the same as for the overall filter with the only exception that the desired function $D_F(\omega)$ and the weighting function $W_F(\omega)$ are not constants in the passband and stopband regions. Therefore, the following $G_1^{(r)}(z)$'s and $G_2^{(r)}(z)$'s can be designed in the same manner. Finally, $F^{(R)}(z)$ is determined at Step 6 like $F(z)$ in one-stage designs.

Given the filter specifications, the remaining problem is to select R as well as the L_r's to minimize the filter complexity. This problem has been considered in [Lim and Lian, 1993]. Assuming that for all the selected L_r's, $\theta + \phi \approx \pi$, the sum of the estimated orders of $F^{(R)}(z)$ and the $G_1^{(r)}(z)$'s and $G_2^{(r)}(z)$'s becomes

$$N_{\text{ove}}(R) = \left[1 \Big/ \prod_{r=1}^{R} L_r + [2(\omega_s - \omega_p)/\pi] \sum_{r=1}^{R} L_r \right] N_{\text{opt}}. \tag{25}$$

The minimum of $N_{\rm ove}(R)$ taking place at

$$L_1 = L_2 = \cdots = L_R = L_{\rm opt}(R) = \left[\frac{2(\omega_s - \omega_p)}{\pi}\right]^{-1/(R+1)} \tag{26}$$

is

$$N_{\rm ove}(R) = (R+1)\left[\frac{2(\omega_s - \omega_p)}{\pi}\right]^{R/(R+1)} N_{\rm opt}. \tag{27}$$

The derivation of the above formula is based on the assumption that the orders of all the $G_1^{(r)}(z)$'s and $G_2^{(r)}(z)$'s for $r = 1, 2, \cdots, R$ are equal, which is seldom true. Therefore, in order to minimize the overall filter complexity, the values of the L_r's should be varied in the vicinity of $L_{\rm opt}(R)$. Given ω_p, ω_s, and R, good values for the L_r's can be obtained by the following procedure:

1. Set $r = 1$.
2. Determine $L = L_{\rm opt}(R + 1 - r)$ from Eq. (26).
3. For values of $\widetilde{L}_r$ in the vicinity of L determine $\theta(\widetilde{L}_r)$ and $\phi(\widetilde{L}_r)$.
4. If $r = R$, then go to Step 7. Otherwise, go to the next step.
5. Determine $L_r = \widetilde{L}_r$ minimizing

$$(R+1-r)\left[\frac{2[\phi(\widetilde{L}_r) - \theta(\widetilde{L}_r)]}{\pi}\right]^{(R-r)/(R+1-r)} + \frac{\phi(\widetilde{L}_r) - \theta(\widetilde{L}_r)}{\theta(\widetilde{L}_r) + \phi(\widetilde{L}_r)} + \frac{\phi(\widetilde{L}_r) - \theta(\widetilde{L}_r)}{2\pi - \theta(\widetilde{L}_r) - \phi(\widetilde{L}_r)}. \tag{28}$$

6. Set $r = r + 1$, $\omega_p = \theta(L_r)$, $\omega_s = \phi(L_r)$, and go to Step 2.
7. Determine $L_R = \widetilde{L}_R$ minimizing

$$\frac{1}{\widetilde{L}_R} + \frac{\phi(\widetilde{L}_R) - \theta(\widetilde{L}_R)}{\theta(\widetilde{L}_R) + \phi(\widetilde{L}_R)} + \frac{\phi(\widetilde{L}_R) - \theta(\widetilde{L}_R)}{2\pi - \theta(\widetilde{L}_R) - \phi(\widetilde{L}_R)}. \tag{29}$$

At the first step in this procedure, L_1 is determined to minimized the estimated overall complexity of $G_1^{(1)}(z)$, $G_2^{(1)}(z)$, and the remaining $F^{(1)}(z)$, which is given by Eq. (28) as a fraction of $N_{\rm opt}$. Compared to Eq. (17) for the one-stage design, $1/\widetilde{L}_r$ is replaced in Eq. (28) by the first term. This term estimates the complexity of $F^{(1)}(z)$ based on the use of Eq. (27) with $\omega_p = \theta(\widetilde{L}_r)$ and $\omega_s = \phi(\widetilde{L}_r)$ and the fact that it is a $R - 1$ stage design. Also, L_2 is redetermined based on the same assumptions and the process is continued in the same manner. Finally, L_R is determined to minimize the sum of the estimated orders of $G_1^{(R)}(z)$, $G_2^{(R)}(z)$, and $F^{(R)}(z)$ like in the one-stage design [cf. Eq. (17)].

Example 2: Consider the specifications of Example 1. For a two-stage design, the above procedure gives $L_1 = L_2 = 6$. For these values, $F^{(0)}(z) \equiv H(z)$ and $F^{(1)}(z)$ are Case A designs ($l = 1$) with $\theta = 0.4\pi$ and $\phi = 0.412\pi$; and $\theta = 0.4\pi$ and $\phi = 0.472\pi$, respectively. The minimum orders of $G_1^{(1)}(z)$, $G_2^{(1)}(z)$, $G_1^{(2)}(z)$, $G_2^{(2)}(z)$, and $F^{(2)}(z)$ are 26, 40, 28, 36, and 74, respectively. Compared with the conventional direct-form FIR filter of order 2541, the number of multipliers and adders required by this design (107 and 204) are only 8 % at the

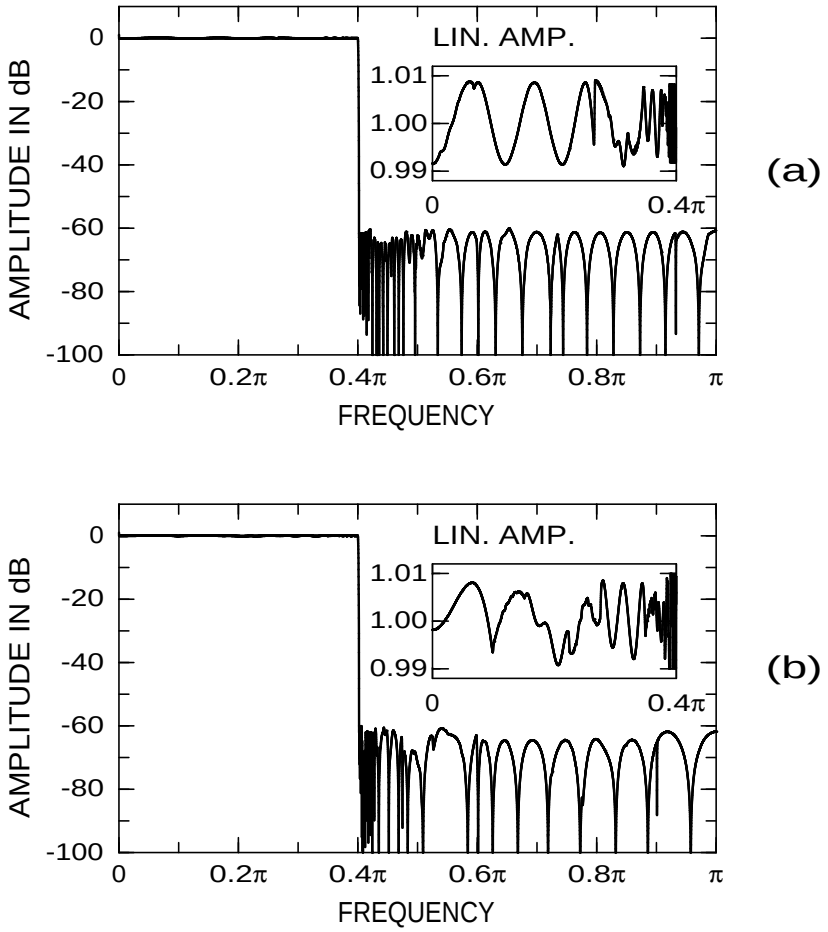

Figure 7 Amplitude responses for filters synthesized using the multistage frequency-response masking approach. (a) Two-stage filter. (b) Three-stage filter.

expense of a 15 % increase in the overall filter order (to 2920). For a three-stage design, we get $L_1 = L_2 = L_3 = 4$. In this case, $F^{(0)}(z)$, $F^{(1)}(z)$, and $F^{(2)}(z)$ are Case B designs ($l = 1$) with $\theta = 0.392\pi$ and $\phi = 0.4\pi$; $\theta = 0.4\pi$ and $\phi = 0.432\pi$; and $\theta = 0.272\pi$ and $\phi = 0.4\pi$, respectively. The minimum orders of $G_1^{(1)}(z)$, $G_2^{(1)}(z)$, $G_1^{(2)}(z)$, $G_2^{(2)}(z)$, $G_1^{(3)}(z)$, $G_2^{(3)}(z)$, and $F^{(3)}(z)$ are 16, 28, 18, 24, 16, 32, and 40, respectively. The number of multipliers and adders (94 and 174) are only 7% of those required by the direct-form equivalent at the expense of a 26 % increase in the overall filter order (to 3196). The amplitude responses of the resulting two-stage and three-stage designs are depicted in Fig. 7.

Design of Narrowband Filters

Another general approach for designing multiplier-efficient FIR filters has been proposed by Jing and Fam [Jing and Fam, 1984]. This design technique is based on iteratively using the fact that there exist efficient implementation forms for filters with $\omega_s < \pi/2$ and for filters with $\omega_p > \pi/2$. A filter with $\omega_s < \pi/2$ is called a *narrowband* filter while that with $\omega_p > \pi/2$ is called a *wideband* filter. This subsection considers the design of narrowband filters, whereas the next subsection is devoted to the design wideband filters. Finally, these techniques are combined, resulting in the Jing-Fam approach.

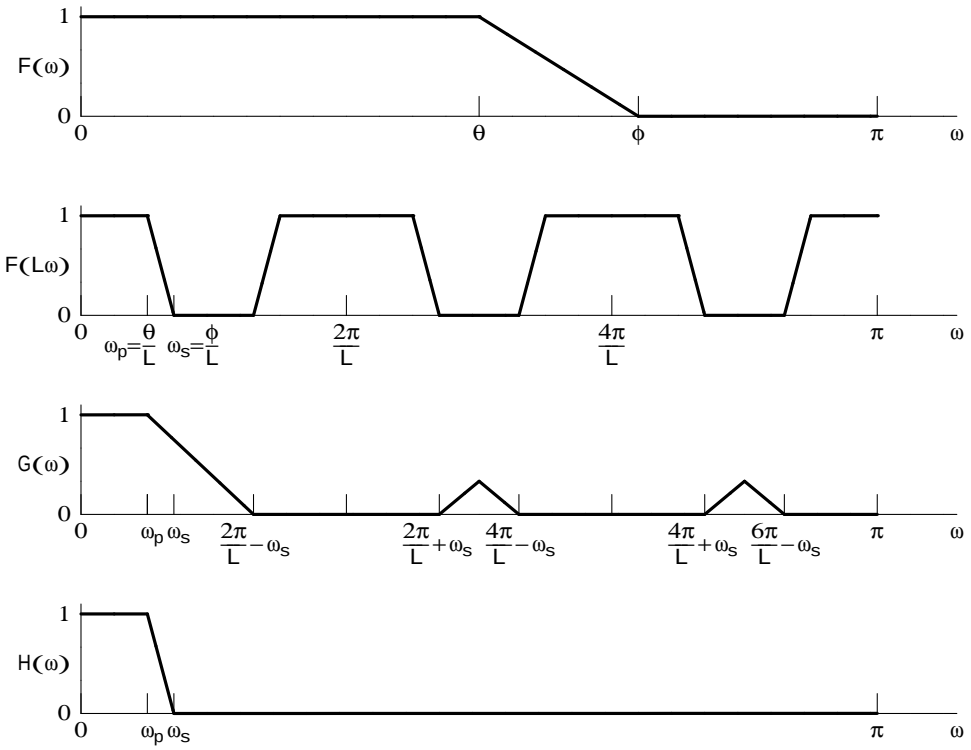

Figure 8 Synthesis of a narrowband filter as a cascade of a periodic and a nonperiodic filter.

When the stopband edge of $H(z)$ is less than $\pi/2$, the first transition band of $F(z^L)$ can be used as that of $H(z)$ (see Fig. 8), that is,

$$\omega_p = \phi/L, \quad \omega_s = \theta/L. \tag{30}$$

In this case, the overall transfer function can be written in the following simplified from [Neuvo, Dong, Mitra, 1984], [Saramäki, Neuvo, Mitra, 1987]:

$$H(z) = F(z^L)G(z), \tag{31}$$

where the orders of both $F(z)$ and $G(z)$ can be freely selected to be either even or odd. As shown in Fig. 8, the role of $G(z)$ is to provide the desired attenuation on those regions where $F(z^L)$ has extra unwanted passband and transition band regions, that is, on

$$\Omega_s(L, \omega_s) = \bigcup_{k=1}^{\lfloor L/2 \rfloor} \Big[k\frac{2\pi}{L} - \omega_s,\ \min(k\frac{2\pi}{L} + \omega_s, \pi) \Big]. \tag{32}$$

There exist two ways of designing the subfilters $F(z^L)$ and $G(z)$. In the first case, they are determined, by means of the Remez algorithm, to satisfy

$$1 - \delta_p^{(F)} \le F(\omega) \le 1 + \delta_p^{(F)} \quad \text{for} \quad \omega \in [0,\ L\omega_p] \tag{33a}$$

$$-\delta_s \le F(\omega) \le \delta_s \quad \text{for} \quad \omega \in [L\omega_s,\ \pi] \tag{33b}$$

$$1 - \delta_p^{(G)} \le G(\omega) \le 1 + \delta_p^{(G)} \quad \text{for} \quad \omega \in [0,\ \omega_p] \tag{33c}$$

$$-\delta_s \le G(\omega) \le \delta_s \quad \text{for} \quad \omega \in \Omega_s(L, \omega_s), \tag{33d}$$

where

$$\delta_p^{(G)} + \delta_p^{(F)} = \delta_p. \tag{33e}$$

The ripples $\delta_p^{(F)}$ and $\delta_p^{(G)}$ can be selected, e.g., to be half the overall ripple δ_p. In the above specifications, both $F(z^L)$ and $G(z)$ have $[0,\ \omega_p]$ as a passband region.

Another approach, leading to a considerable reduction in the order of $G(z)$, is to design simultaneously $F(\omega)$ to satisfy

$$1 - \delta_p \le F(\omega)G(\omega/L) \le 1 + \delta_p \quad \text{for} \quad \omega \in [0,\ L\omega_p] \tag{34a}$$

$$-\delta_s \le F(\omega)G(\omega/L) \le \delta_s \quad \text{for} \quad \omega \in [L\omega_s,\ \pi] \tag{34b}$$

and $G(\omega)$ to satisfy

$$G(0) = 1 \tag{35a}$$

$$-\delta_s \le F(L\omega)G(\omega) \le \delta_s \quad \text{for} \quad \omega \in \Omega_s(L, \omega_s). \tag{35b}$$

The desired overall solution can be obtained by iteratively determining, by means of the Remez algoritm, $F(z)$ to meet the criteria of Eq. (34) and $G(z)$ to meet the criteria of Eq. (35). Typically, only three to five designs of both of the subfilters are required to arrive at a solution which does not change if further iterations are used. For more details, see [Saramäki, Neuvo, Mitra, 1987] or [Saramäki, 1993]. Figure 9 shows typical responses for $G(z)$ and $F(z^L)$ and for the overall optimized design. As seen in this figure, $G(z)$ has all its zeros on the unit circle concentrating on providing the desired attenuation for the overall response on $\Omega_s(L, \omega_s)$, whereas $F(z^L)$ makes the overall response equiripple in the passband and in the stopband portion $[\omega_s,\ \pi/L]$.

For the order of $F(z)$, a good estimate is

$$N_F \approx \frac{\Phi(\delta_p, \delta_s)/L}{\omega_s - \omega_p}, \tag{36}$$

so that it is $1/L$th of that of an optimum conventional nonperiodic filter meeting the given overall criteria. The order of $G(z)$, in turn, can be estimated accurately by [Saramäki, 1993]

$$N_G = \cosh^{-1}(1/\delta_s)\left[\frac{1}{X\left(\omega_p, \frac{2\pi}{L} - \frac{\omega_p + 2\omega_s}{3}\right)} + \frac{L/2}{X\left(\frac{L\omega_p}{2}, \pi - \frac{L(\omega_p + 2\omega_s)}{6}\right)}\right], \tag{37a}$$

where

$$X(\omega_1, \omega_2) = \cosh^{-1}\Big[(2\cos\omega_1 - \cos\omega_2 + 1)/(1 + \cos\omega_2)\Big]. \tag{37b}$$

The minimization of the number of multipliers, $\lfloor (N_F + 2)/2 \rfloor + \lfloor (N_F + 2)/2 \rfloor$, with respect to L can be performed conveniently by evaluating the sum of the above estimated orders for admissible values of L, $2 \le L < \pi/\omega_s$. The upper limit is a consequence of the fact that the stopband edge angle of $F(z)$, $\phi = L\omega_s$, must be less than π. The following example illustrates the minimization of the filter complexity.

Example 3. The narrowband specifications are $\omega_p = 0.025\pi$, $\omega_s = 0.05\pi$, $\delta_p = 0.01$, and $\delta_s = 0.001$. Figure 10(a) shows the estimated N_F, N_G, and $N_F + N_G$ as functions of L, whereas Fig. 10(b) shows the corresponding actual minimum orders. It is seen that

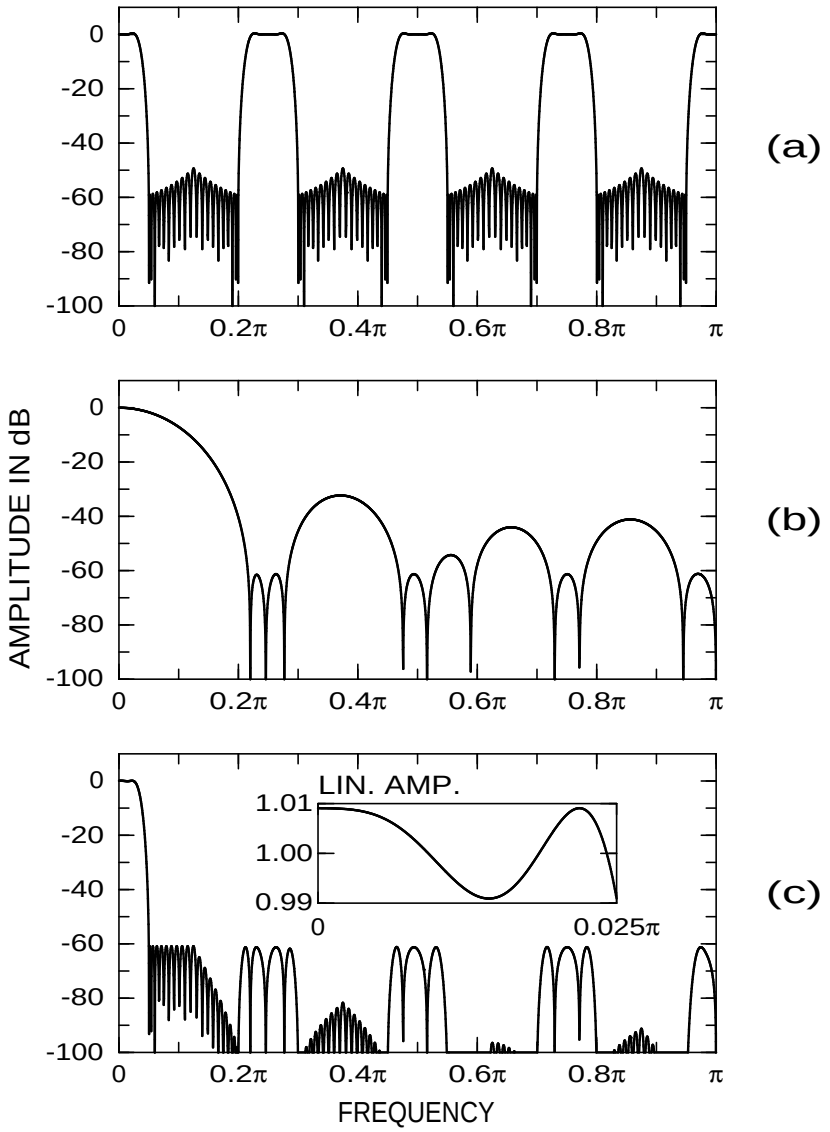

Figure 9 Typical amplitude responses for a filter of the form $H(z) = F(z^L)G(z)$. $L = 8$, $\omega_p = 0.025\pi$, $\omega_s = 0.05\pi$, $\delta_p = 0.01$, and $\delta_s = 0.001$. (a) $F(z^L)$ of order 26 in z^L. (b) $G(z)$ of order 19. (c) Overall filter.

the estimated orders are so close to the actual ones that the minimization of the filter complexity can be accomplished based on the use of the above estimation formulas. It is also observed that $N_F + N_G$ is a unimodal function of L. With the estimates, $L = 8$ gives the best result. The estimated orders are $N_F = 25$ and $N_G = 19$, whereas the actual orders are $N_F = 26$ and $N_G = 19$. The amplitude responses for the subfilters and for the overall filter are depicted in Fig. 9. This design requires 24 multipliers and 45 adders. The minimum order of a conventional direct-form design is 216, requiring 109 multipliers and 216 adders. The price paid for these 80 % reductions in the filter complexity is a 5 % increase in the overall filter order (from 216 to 227).

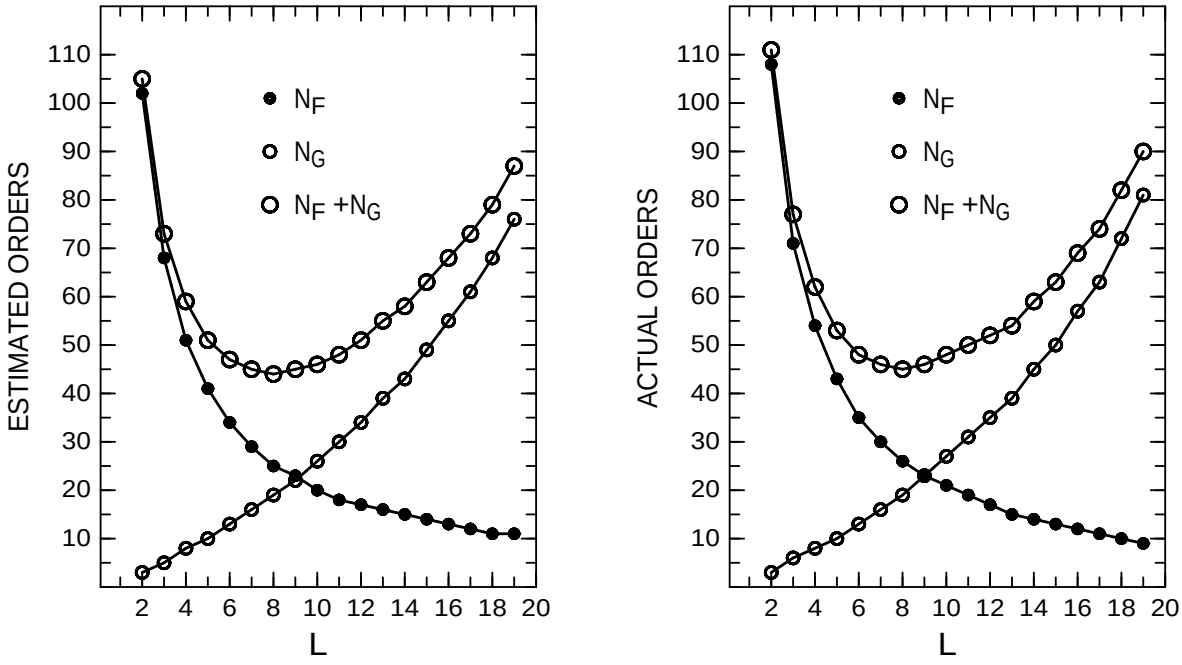

Figure 10 Estimated and actual subfilter orders as well as the sum of the subfilter orders verus L in a typical narrowband case.

In the cases where L can be factored into the product

$$L = \prod_{r=1}^{R} L_r, \tag{38}$$

where the L_r's are integers, further savings in the filter complexity can be achieved by designing $G(z)$ in the following multistage form [Saramäki, Neuvo, Mitra, 1988]:

$$G(z) = G_1(z)G_2(z^{L_1})G_3(z^{L_1L_2})\cdots G_K(z^{L_1L_2\cdots L_{R-1}}). \tag{39}$$

Another alternative to reduce the number of adders and multipliers is to use special structures for implementing $G(z)$ [Saramäki, Neuvo, Mitra, 1988], [Saramäki, Fam, 1988], [Saramäki, 1993].

Design of Wideband Filters

The synthesis of a wideband filter $H(z)$ can be converted into the design of a narrowband filter based on the following fact. If $\widehat{H}(z)$ of even-order $2M$ is lowpass design with the following edges and ripples:

$$\widehat{\omega}_p = \pi - \omega_s, \quad \widehat{\omega}_s = \pi - \omega_p, \quad \widehat{\delta}_p = \delta_s, \quad \widehat{\delta}_s = \delta_p, \tag{40}$$

then

$$H(z) = z^{-M} - (-1)^M \widehat{H}(-z) \tag{41}$$

is a lowpass filter having the passband and stopband edge angles at ω_p and ω_s and the passband and stopband ripples of δ_p and δ_s. Hence, if ω_p and ω_s of $H(z)$ are larger than

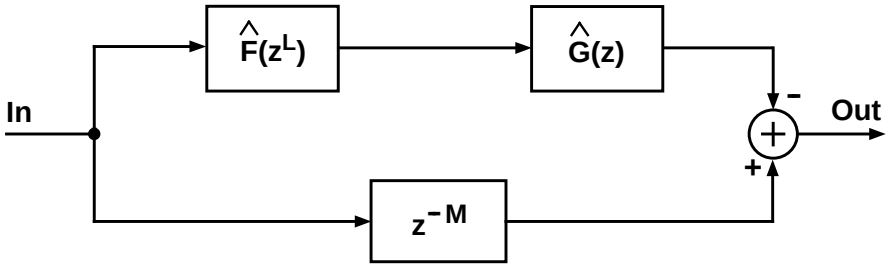

Figure 11 Implementation for a wideband filter in the form $H(z) = z^{-M} - (-1)^M F((-z)^L)G(-z)$. $\widehat{F}(z^L) = (-1)^M F((-z)^L)$ and $\widehat{G}(z) = G(-z)$.

$\pi/2$, then $\widehat{\omega}_p$ and $\widehat{\omega}_s$ of $\widehat{H}(z)$ are smaller than $\pi/2$. This enables us to design $\widehat{H}(z)$ in the form

$$\widehat{H}(z) = F(z^L)G(z) \tag{42}$$

using the techniques of the previous subsection, yielding

$$H(z) = z^{-M} - (-1)^M F((-z)^L)G(-z), \tag{43a}$$

where

$$M = (LN_F + N_G)/2 \tag{43b}$$

is half the order of $F(z^L)G(z)$. For implementation purposes, $H(z)$ is expressed as

$$H(z) = z^{-M} - \widehat{F}(z^L)\widehat{G}(z), \quad \widehat{F}(z^L) = (-1)^M F((-z)^L), \quad \widehat{G}(z) = G(-z). \tag{44}$$

An implementation of this transfer function is shown in Fig. 11, where the delay term z^{-M} can be shared with $\widehat{F}(z^L)$. To avoid half-sample delays, the order of $\widehat{F}(z^L)\widehat{G}(z)$ has to be even.

Example 4: The wideband specifications are $\omega_p = 0.95\pi$, $\omega_s = 0.975\pi$, $\delta_p = 0.001$, and $\delta_s = 0.01$. From Eq. (40), the specifications of $\widehat{H}(z)$ become $\widehat{\omega}_p = 0.025\pi$, $\widehat{\omega}_s = 0.05\pi$, $\widehat{\delta}_p = 0.01$, and $\widehat{\delta}_s = 0.001$. These are the narrowband specifications of Example 3. The desired wideband design is thus obtained by using the subfilters $F(z^L)$ and $G(z)$ of Fig. 9 ($L = 8$, $N_F = 26$, and $N_G = 19$). However, the overall order is odd (227). A solution with even order is achieved by increasing the order of $G(z)$ by one ($N_G = 20$). Figure 12 shows the amplitude response of the resulting filter, requiring 25 multipliers, 46 adders, and 228 delay elements. The corresponding numbers for a conventional direct-form equivalent of order 216 are 109, 216, and 216, respectively.

Generalized Designs

The Jing-Fam approach [Jing and Fam, 1984] is based on iteratively using the facts that a narrowband filter can be implemented effectively as $H(z) = F(z^L)G(z)$ and a wideband filter in the form of Eq. (43). In this approach, a narrowband filter is generated as [Saramäki and Fam, 1988]

$$H(z) \equiv \widehat{H}_1(z) = G_1(z)F_1(z^{L_1}), \tag{45a}$$

where

$$F_1(z) = z^{-M_1} - (-1)^{M_1}\widehat{H}_2(-z), \quad \widehat{H}_2(z) = G_2(z)F_2(z^{L_2}) \tag{45b}$$

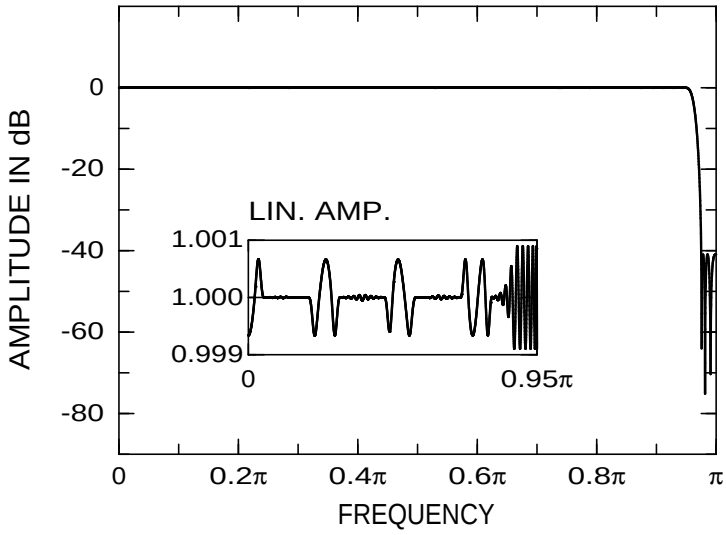

Figure 12 Amplitude response for a wideband filter implemented as shown in Fig. 11.

$$F_2(z) = z^{-M_2} - (-1)^{M_2}\widehat{H}_3(-z), \quad \widehat{H}_3(z) = G_3(z)F_3(z^{L_3}) \tag{45c}$$

$$\vdots \quad \vdots \quad \vdots$$

$$F_{R-2}(z) = z^{-M_{R-2}} - (-1)^{M_{R-2}}\widehat{H}_{R-1}(-z), \quad \widehat{H}_{R-1}(z) = G_{R-1}(z)F_{R-1}(z^{L_{R-1}}) \tag{45d}$$

$$F_{R-1}(z) = z^{-M_{R-1}} - (-1)^{M_{R-1}}\widehat{H}_R(-z), \quad \widehat{H}_R(z) = G_R(z), \tag{45e}$$

with M_r for $r = 1, 2, \cdots, R-1$ being half the order of $\widehat{H}_{r+1}(z)$. Here, the basic idea is to convert iteratively the design of the narrowband overall filter into the designs of narrowband transfer functions $\widehat{H}_r(z)$ for $r = 2, 3, \cdots, R$ until the transition bandwidth of the remaining $\widehat{H}_R(z) = G_R(z)$ becomes large enough and, correspondingly, its complexity (the number of multipliers) is low enough. The desired conversion is performed by properly selecting the L_r's and designing the low-order filters $G_r(z)$ for $r = 1, 2, \cdots, R-1$.

In order to determine the conditions for the L_r's as well as the design criteria for the $G_r(z)$'s, we consider the rth iteration, where

$$\widehat{H}_r(z) = G_r(z)F_r(z^{L_r}) \tag{46a}$$

with

$$F_r(z) = z^{-M_r} - (-1)^{M_r}\widehat{H}_{r+1}(-z). \tag{46b}$$

Let the ripples of $\widehat{H}_r(z)$ be $\widehat{\delta}_p^{(r)}$ and $\widehat{\delta}_s^{(r)}$ and the edges be located at $\omega_p^{(r)} < \pi/2$ and $\omega_s^{(r)} < \pi/2$. Since $F_r(z)$ is implemented in the form of Eq. (46b), it cannot alone take care of shaping the passband response of $\widehat{H}_r(z)$. Therefore, the simultaneous criteria for $G_r(z)$ and $F_r(z)$ are stated according to Eq. (33) so that the passband and stopband regions of $G_r(z)$ are, respectively, $[0,\ \omega_p^{(r)}]$ and $\Omega_s(L_r, \omega_s^{(r)})$ with $\Omega_s(L, \omega_s)$ given by Eq. (32). L_r has to be determined such that the edges of $F_r(z)$, $L_r\omega_p^{(r)}$ and $L_r\omega_s^{(r)}$, become larger than $\pi/2$ and, correspondingly, the edges of $\widehat{H}_{r+1}(z)$, $\omega_p^{(r+1)} = \pi - L_r\omega_s^{(r)}$ and $\omega_p^{(r+1)} = \pi - L_r\omega_s^{(r)}$, become less than $\pi/2$.

In the case of the specifications of Eq. (33), the stopband ripple of $G_r(z)$, denoted for later use by $\delta_s^{(r)}$, and that of $F_r(z)$ are equal to $\widehat{\delta}_s^{(r)}$, whereas the sum of the passband ripples is equal to $\widehat{\delta}_p^{(r)}$. Denoting by $\delta_p^{(r)}$ the passband ripple selected for $G_r(z)$, the corresponding ripple of $F_r(z)$ is $\widehat{\delta}_p^{(r)} - \delta_p^{(r)}$. Since $F_r(z)$ and $\widehat{H}_{r+1}(z)$ interchange the ripples, the ripple requirements for $\widehat{H}_{r+1}(z)$ are $\widehat{\delta}_p^{(r+1)} = \widehat{\delta}_s^{(r)}$ and $\widehat{\delta}_s^{(r+1)} = \widehat{\delta}_p^{(r)} - \delta_p^{(r)}$.

The criteria for the $G_r(z)$'s for $r = 1, 2, \cdots, R$, can thus be stated as

$$1 - \delta_p^{(r)} \le G_r(\omega) \le 1 + \delta_p^{(r)} \quad \text{for} \quad \omega \in [0,\ \omega_p^{(r)}] \tag{47a}$$

$$-\delta_s^{(r)} \le G_r(\omega) \le \delta_s^{(r)} \quad \text{for} \quad \omega \in \Omega_s^{(r)}, \tag{47b}$$

where

$$\Omega_s^{(r)} = \begin{cases} \bigcup\limits_{k=1}^{\lfloor L_r/2 \rfloor} \left[k\dfrac{2\pi}{L_r} - \omega_s^{(r)},\ \min(k\dfrac{2\pi}{L_r} + \omega_s^{(r)}, \pi) \right] & \text{for } r < R \\ [\omega_s^{(R)},\ \pi] & \text{for } r = R. \end{cases} \tag{47c}$$

Here, the $\omega_p^{(r)}$'s and $\omega_s^{(r)}$'s for $r = 2, 3, \cdots, R$ are determined iteratively as

$$\omega_p^{(r)} = \pi - L_{r-1}\omega_s^{(r-1)}, \quad \omega_s^{(r)} = \pi - L_{r-1}\omega_p^{(r-1)}, \tag{47d}$$

where $\omega_p^{(1)} = \omega_p$ and $\omega_s^{(1)} = \omega_s$ are the edges of the overall design, and the $\delta_s^{(r)}$'s as

$$\delta_s^{(r)} = \begin{cases} \delta_p - \sum\limits_{\substack{k=1 \\ k \text{ odd}}}^{r-1} \delta_p^{(k)} & \text{for } r \text{ even} \\ \delta_s - \sum\limits_{\substack{k=2 \\ k \text{ even}}}^{r-1} \delta_p^{(k)} & \text{for } r \text{ odd}, \end{cases} \tag{47e}$$

where δ_p and δ_s are the ripple values of the overall filter and $\delta_p^{(r)}$ is the passband ripple selected for $G_r(z)$. In order for the overall filter to meet the given ripple requirements, $\delta_s^{(R)}$ and the $\delta_p^{(r)}$'s have to satisfy for R even

$$\sum_{\substack{k=2 \\ k \text{ even}}}^{R} \delta_p^{(k)} = \delta_s, \quad \delta_s^{(R)} + \sum_{\substack{k=1 \\ k \text{ odd}}}^{R-1} \delta_p^{(k)} = \delta_p \tag{48a}$$

or for R odd

$$\sum_{\substack{k=1 \\ k \text{ odd}}}^{R} \delta_p^{(k)} = \delta_p, \quad \delta_s^{(R)} + \sum_{\substack{k=2 \\ k \text{ even}}}^{R-1} \delta_p^{(k)} = \delta_s. \tag{48b}$$

In the above, the L_r's have to be determined such that the $\omega_s^{(r)}$'s for $r < R$ become smaller than $\pi/2$. It is also desired that for the last filter stage $G_R(z)$, $\omega_s^{(R)}$ is smaller than $\pi/2$.

If $2\pi/L_r - \omega_s^{(r)} < \pi/2$ for $r < R$ or $\omega_s^{(R)} < \pi/2$, then the arithmetic complexity of $G_r(z)$ can be reduced by designing it, using the techniques of previous subsections, in the form

$$G_r(z) = G_r^{(1)}(z^{K_r})G_r^{(2)}(z). \tag{49}$$

It is preferred to design the subfilters of $G_r(z)$ in such a way that the passband shaping is done entirely by $G_r^{(1)}(z^{K_r})$. The number of multipliers in the $G_r(z)$'s for $r = 1, 2, \cdots, R-1$ can be reduced by the experimentally observed fact that the overall filter still meets the given criteria when the stopband regions of these filters are decreased by using in Eq. (47c) the substitution

$$(2\omega_s^{(r)} + \omega_p^{(r)})/3 \mapsto \omega_s^{(r)}. \tag{50}$$

After some manipulations, $H(z)$ as given by Eqs. (45) and (49) can be rewritten in the explicit form shown in Table 4. If $G_r(z)$ is a single-stage design, then $G_r^{(1)}(z^{K_r}) \equiv 1$. In order to obtain the desired overall solution, the overall order of $G_r(z)$ for $r \geq 2$, denoted by N_r in Table 4, has to be even. Realizations for the overall transfer function are given Fig. 13, where

$$m_r = \widehat{M}_r - \widehat{M}_{r+1} = \frac{1}{2}\widehat{L}_r N_r, \quad r = 2, 3, \cdots, R-1, \quad m_R = \widehat{M}_R. \tag{51}$$

The structure of Fig. 13(b) is preferred since the delay terms z^{-m_r} can be shared with $H_R^{(1)}(z^{K_R\widehat{L}_R})$ or, if this filter stage is not present, with $H_R^{(2)}(z^{\widehat{L}_R})$. This is because the overall order of this filter stage is usually larger than the sum of the m_r's.

If the edges ω_p and ω_s of the overall filter are larger than $\pi/2$, then we set $H(z) \equiv F_1(z)$. In this case, $\delta_p^{(1)} \equiv 0$, $L_1 \equiv 1$, and $G_1(z)$, $\omega_p^{(1)}$, and $\omega_s^{(1)}$ are absent. Furthermore, $\omega_p^{(2)} = \pi - \omega_s$ and $\omega_s^{(2)} = \pi - \omega_p$, and $H_1(z)$ is absent in Fig. 13 and in Table 4.

The remaining problem is to select R, the L_r's, the K_r's, and the ripple values such that the filter complexity is minimized. The following example illustrates this.

Example 5: Consider the specifications of Example 1, that is, $\omega_p = 0.4\pi$, $\omega_s = 0.402\pi$, $\delta_p = 0.01$, $\delta_s = 0.001$. In this case, the only alternative is to select $L_1 = 2$. The resulting passband and stopband regions for $G_1(z)$ are (the substitution of Eq. (50) is used)

$$\Omega_p^{(1)} = [0,\ 0.4\pi], \quad \Omega_s^{(1)} = [0.5987\pi,\ \pi].$$

For $\widehat{H}_2(z)$, the edges become $\omega_p^{(2)} = \pi - L_1\omega_s = 0.196\pi$ and $\omega_s^{(2)} = \pi - L_1\omega_p = 0.2\pi$. For L_2, there are two alternatives to make the edges of $\widehat{H}_3(z)$, $\omega_p^{(3)} = \pi - L_2\omega_s^{(2)}$ and $\omega_s^{(3)} = \pi - L_2\omega_p^{(2)}$, less than $\pi/2$. These are $L_2 = 3$ and $L_2 = 4$. For $R = 5$ stages, there are the following four alternatives to make all the the $\omega_s^{(r)}$'s smaller than $\pi/2$:

$$L_1 = 2, \quad L_2 = 4, \quad L_3 = 3, \quad L_4 = 2$$

$$L_1 = 2, \quad L_2 = 4, \quad L_3 = 4, \quad L_4 = 4$$

$$L_1 = 2, \quad L_2 = 3, \quad L_3 = 2, \quad L_4 = 4$$

Table 4 Explicit Form for the Transfer function in the Jing-Fam Approach

$$H(z) = H_1(z^{\widehat{L}_1})[I_2 z^{-\widehat{M}_2} + H_2(z^{\widehat{L}_2})[I_3 z^{-\widehat{M}_3} + H_3(z^{\widehat{L}_3})[\cdots$$

$$[I_{R-1} z^{-\widehat{M}_{R-1}} + H_{R-1}(z^{\widehat{L}_{R-1}})[I_R z^{-\widehat{M}_R} + H_R(z^{\widehat{L}_R})]]\cdots]]],$$

where

$$H_r(z^{\widehat{L}_r}) = H_r^{(1)}(z^{K_r \widehat{L}_r}) H_r^{(2)}(z^{\widehat{L}_r})$$

$$H_r^{(1)}(z) = G_r^{(1)}(J_r^{(1)} z), \quad H_r^{(2)}(z) = S_r G_r^{(2)}(J_r^{(2)} z)$$

$$S_1 = 1, \quad S_r = -(-1)^{\widehat{M}_r/\widehat{L}_r}, \quad r = 2, 3, \cdots, R$$

$$J_1^{(2)} = 1, \quad J_2^{(2)} = -1, \quad J_r^{(2)} = -[J_{r-1}^{(2)}]^{L_{r-1}}, \quad r = 3, 4, \cdots, R$$

$$J_r^{(1)} = [J_r^{(2)}]^{K_r}$$

$$\widehat{L}_1 = 1, \quad \widehat{L}_r = \prod_{k=1}^{r-1} L_k, \ r = 2, 3, \cdots, R$$

$$\widehat{M}_R = \tfrac{1}{2}\widehat{L}_R N_R, \quad \widehat{M}_{R-r} = \widehat{M}_{R-r+1} + \tfrac{1}{2}\widehat{L}_{R-r} N_{R-r}, \quad r = 1, 2, \cdots, R-2$$

$$I_2 = 1, \quad I_r = [J_{r-1}^{(2)}]^{\widehat{M}_r/\widehat{L}_{r-1}}, \quad r = 3, 4, \cdots, R$$

$$N_r = K_r N_r^{(1)} + N_r^{(2)}$$

$N_r^{(1)}$ and $N_r^{(2)}$ are the orders of $G_r^{(1)}(z)$ and $G_r^{(2)}(z)$, respectively.

$$L_1 = 2, \quad L_2 = 3, \quad L_3 = 2, \quad L_4 = 3.$$

Among these alternatives, the first one results in an overall filter with minimum complexity. In this case, the edges of $\widehat{H}_3(z)$, $\widehat{H}_4(z)$, and $\widehat{H}_5(z) \equiv G_5(z)$ become as shown in Table 5. The corresponding passband and stopband regions for $G_2(z)$, $G_3(z)$, $G_4(z)$, and $G_5(z)$ are

$$\Omega_p^{(2)} = [0,\ 0.196\pi], \quad \Omega_s^{(2)} = [0.3013\pi,\ 0.6987\pi] \cup [0.8013\pi,\ \pi],$$

$$\Omega_p^{(3)} = [0,\ 0.2\pi], \quad \Omega_s^{(3)} = [0.4560\pi,\ 0.8773\pi],$$

$$\Omega_p^{(4)} = [0,\ 0.352\pi], \quad \Omega_s^{(4)} = [0.616\pi,\ \pi],$$

$$\Omega_p^{(5)} = [0,\ 0.2\pi], \quad \Omega_s^{(5)} = [0.296\pi,\ \pi].$$

What remains is to determine the ripple requirements. From Eq. (48b), it follows for $R = 5$, $\delta_p^{(1)} + \delta_p^{(3)} + \delta_p^{(5)} = \delta_p$ and $\delta_p^{(2)} + \delta_p^{(4)} + \delta_s^{(5)} = \delta_s$. By simply selecting the ripple values in these summations to be equal, the required ripples for the $G_r(z)$'s become as shown in Table 5.

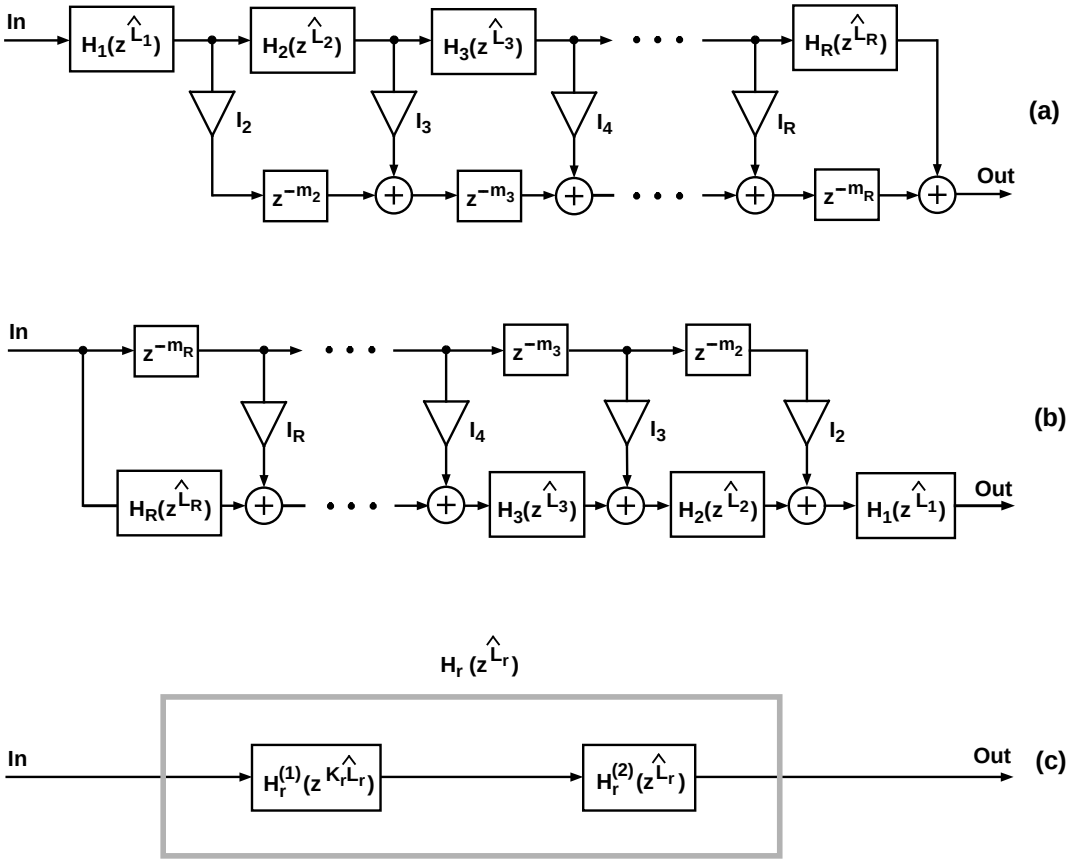

Figure 13 Implementations for a filter synthesized using the Jing-Fam approach. (a) Basic structure. (b) Transposed structure. (c) Structure for the subfilter $H_r(z^{\widehat{L}_r})$.

The first and fourth subfilters are single-stage filters since their stopband edges are larger than $\pi/2$, whereas the remaining three filters are two-stage designs. The parameters describing the overall filter are shown in Table 5, whereas Fig. 14(a) depicts the response of this filter. The number of multipliers and the order of this design are 78 and 4875, whereas the corresponding numbers for the direct-form equivalent are 1271 and 2541. The number of multipliers required by the proposed design is thus only 6 % of that of the direct-form filter. Since the complexity of $H_5(z^{\widehat{L}_5})$ is similar to those of the earlier filter stages, $R = 5$ is a good selection in this example.

The overall filter order as well as the number of multipliers can be decreased by selecting smaller ripple values for the first stages, thereby allowing larger ripples for the last stages. Proper selections for the ripple requirements and filter orders are shown in Table 6. The first four filters have been optimized such that their passband variations are minimized. The first criteria are met by a half-band filter of order 34, having the passband and stopband edges at 0.4013π and 0.5987π. Since every second impulse response coefficient of this filter is zero-valued except for the central coefficient with an easily implementable value of 1/2, this filter requires only 9 multipliers. For the last stage, K_5 is reduced to 2 to decrease the overall filter order. The order of the resulting overall filter [see Fig. 14(b)] is 3914, which is 54 percent higher than that of the direct-form equivalent. The number of multipliers is

Table 5 Data for a Filter Designed Using the Jing-Fam Approach

	$r=1$	$r=2$	$r=3$	$r=4$	$r=5$
$\omega_p^{(r)}$	0.4π	0.196π	0.2π	0.352π	0.2π
$\omega_s^{(r)}$	0.402π	0.2π	0.216π	0.4π	0.296π
$\delta_p^{(r)}$	$\frac{1}{3}\times 10^{-2}$	$\frac{1}{3}\times 10^{-3}$	$\frac{1}{3}\times 10^{-2}$	$\frac{1}{3}\times 10^{-3}$	$\frac{1}{3}\times 10^{-2}$
$\delta_s^{(r)}$	10^{-3}	$\frac{2}{3}\times 10^{-2}$	$\frac{2}{3}\times 10^{-3}$	$\frac{1}{3}\times 10^{-2}$	$\frac{1}{3}\times 10^{-3}$
L_r	2	4	3	2	—
K_r	—	3	2	—	3
$N_r^{(1)}$	—	20	11	—	22
$N_r^{(2)}$	31	10	8	26	14
N_r	31	70	30	26	80
$\widehat{L}_r$	1	2	8	24	48
$J_r^{(1)}$	—	-1	1	—	-1
$J_r^{(2)}$	1	-1	-1	1	-1
$\widehat{M}_r$	—	2422	2352	2232	1920
I_r	—	1	1	-1	1
S_r	1	1	-1	1	-1
m_r	—	70	120	312	1920

reduced to 70.

The above Jing-Fam approach cannot be applied directly for synthesizing filters whose edges are very close to $\pi/2$. This problem can, however, be overcome by slightly changing the sampling rate or, if this not possible, by shifting the edges by a factor of $\frac{3}{2}$ by using decimation by this factor at the filter input and interpolation by the same factor at the filter output [Jing and Fam, 1984]. One attractive feature of the Jing-Fam approach is that it can be combined with multirate filtering to reduce the filter complexity even further [Ramstad and Saramäki, 1990].

When comparing the above designs with the filters synthesized using the multistage frequency-response masking technique (Example 2), it is observed that the above designs require slightly fewer multipliers at the expense of an increased overall filter order. Both of these general approaches are applicable those specifications that are not very narrowband or very wideband. For most very narrowband and wideband cases, filters synthesized in the simplified forms $H(z)=F(z^L)G(z)$ and $H(z)=z^{-M}-F((-z)^L)G(-z)$, respectively, give the best results (see Examples 3 and 4).

Table 6 Data for Another Filter Designed Using the Jing-Fam Approach

$\delta_p^{(r)}$	7.3×10^{-4}	7.1×10^{-5}	3.5×10^{-4}	12.1×10^{-5}	89.2×10^{-4}
$\delta_s^{(r)}$	10^{-3}	92.7×10^{-4}	92.9×10^{-5}	89.2×10^{-4}	80.8×10^{-5}
K_r	—	3	2	—	2
$N_r^{(1)}$	—	22	13	—	27
$N_r^{(2)}$	34	10	8	24	6

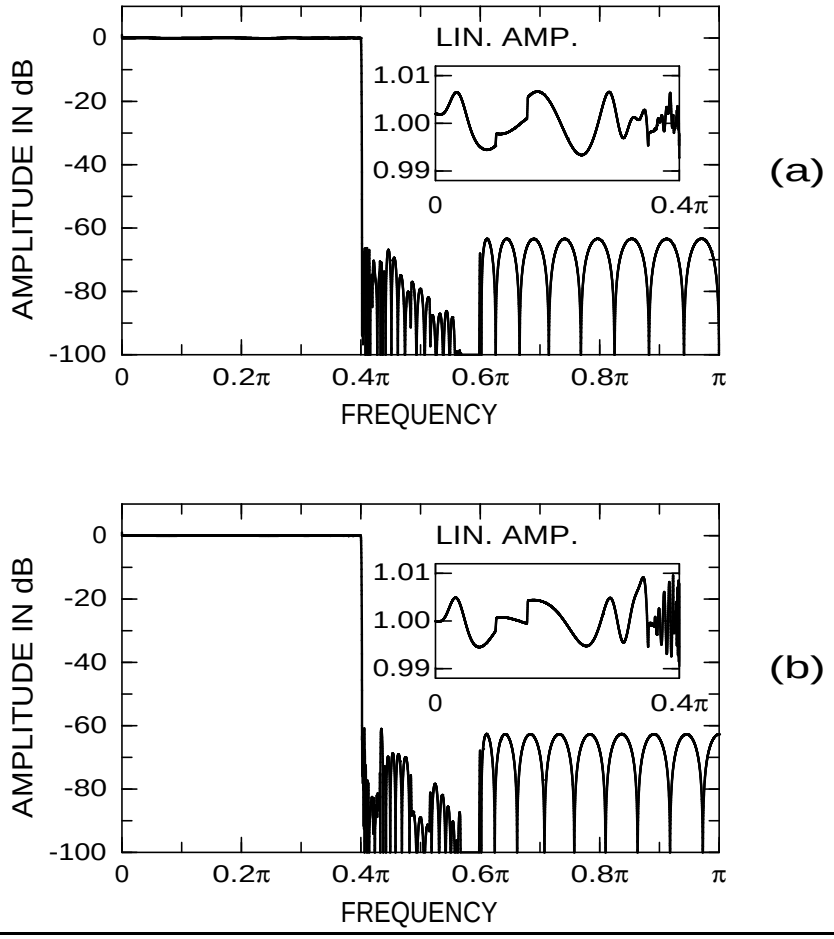

Figure 14 Amplitude responses for filters synthesized using the Jing-Fam approach.

References

Herrmann, O., Rabiner, L. R., and Chan, D. S. K., 1973. "Practical design rules for optimum finite impulse response lowpass digital filters," *Bell System Techical Journal*, vol. 52 (July-August), pp. 769–799.

Jing, Z. and Fam, A. T., 1983. "A new structure for narrow transition band, lowpass digital filter design," *IEEE Transactions on Acoustics, Speech, and Signal Processing,* vol. ASSP-32 (April) , pp. 362-370.

Lim, Y. C., 1986. "Frequency-response masking approach for the synthesis of sharp linear phase digital filters," *IEEE Transactions on Circuits and Systems*, vol. CAS-33 (April), pp. 357–364.

Lim, Y. C., and Lian, Y. 1993. "The optimum design of one- and two-dimensional FIR filters using the frequency response masking technique," *IEEE Transactions on Circuits and Systems — II: Analog and Digital Signal Processing*, vol. 40 (February), pp. 88–95.

McClellan, J. H., Parks, T. W., and Rabiner, L. R. 1973. "A computer program for designing optimum FIR linear phase digital filters," *IEEE Transactions on Audio and Electroacoustics*, vol. AU-21 (December), pp. 506–526; also reprinted in *Selected Papers in Digital Signal Processing, II,* Digital Signal Processing Committee and IEEE ASSP, Eds., IEEE Press, New York, 1975, pp. 97–117.

Neuvo, Y., Dong, C.-Y., and Mitra, S. K., 1984. "Interpolated finite impulse response filters," *IEEE Transactions on Acoustics, Speech, and Signal Processing,* vol. ASSP-32 (June) , pp. 563–570.

Ramstad, T. and Saramäki, T., 1990. "Multistage, multirate FIR filter structures for narrow transition-band filters," in *Proceedings of the 1990 IEEE International Symposium on Circuits and Systems*, New Orleans, Lousiana, pp. 2017–2021.

Saramäki, T., Neuvo, Y., and Mitra, S. K., 1988. "Design of computationally efficient interpolated FIR filters," *IEEE Transactions on Circuits and Systems*, vol. CAS-35 (January), pp. 70–88.

Saramäki, T., and Fam, A. T., 1988. "Subfilter approach for designing efficient FIR filters," in *Proceedings of the 1988 IEEE International Symposium on Circuits and Systems*, Espoo, Finland, pp. 2903–2915.

Saramäki, T., 1993. "Finite impulse reponse filter design", Chapter 4 in *Handbook for Digital Signal Processing*, S. K. Mitra and J. F. Kaiser, Eds., John Wiley and Sons, New York, 1993, pp. 155–277.